Radio Science

RESEARCH ARTICLE
10.1029/2022RS007433

Quantum Based Particle Swarm Optimization for Equivalent Circuit Design of Terminal Antenna Impedance

L. Mescia[1], G. Mevoli[1], and P. Bia[2]

[1]Department of Electric and Information Engineering, Politecnico di Bari, Bari, Italy, [2]Design Solution Department, Elettronica SpA, Rome, Italy

Key Points:

- Quantum–inspired PSO for solving complex electromagnetic problems
- Lumped element equivalent circuit for modeling the driving point antenna impedance
- Effective methodology for synthesising broadband equivalent circuits

Correspondence to:

L. Mescia,
luciano.mescia@poliba.it

Citation:

Mescia, L., Mevoli, G., & Bia, P. (2022). Quantum based particle swarm optimization for equivalent circuit design of terminal antenna impedance. *Radio Science*, *57*, e2022RS007433. https://doi.org/10.1029/2022RS007433

Received 22 JAN 2022
Accepted 23 APR 2022

Author Contributions:

Conceptualization: L. Mescia
Data curation: L. Mescia
Formal analysis: L. Mescia, P. Bia
Investigation: G. Mevoli
Methodology: L. Mescia
Software: P. Bia
Validation: G. Mevoli
Visualization: L. Mescia
Writing – original draft: L. Mescia

Abstract In this paper, an improved quantum-behaved particle swarm optimization (QPSO) approach for modeling antenna impedance is illustrated. In the proposed study, the enhanced weighted quantum particles swarm optimization (EWQPSO) is introduced with the aim to achieve local convergence acting on a reduced number of free parameters. To verify the performance of the proposed EWQPSO, several tests involving Ipersphere, Alpine, De Jong, Zakharov, Salomon functions were carried out. The obtained results demonstrated that the convergence is achieved more quickly by the EWPSO than other optimization algorithms based on QPSO. A lumped element equivalent circuit was designed to model the terminal impedance of a broadband planar sinuous antenna in the frequency range from 1 to 3 GHz. The developed EWQPSO algorithm is then used to recover all the parameters characterizing the equivalent circuit. The resulting circuit exhibited a good impedance fidelity over the whole frequency range.

1. Introduction

The microwave and antenna systems designers are constantly involved in the optimal design of electromagnetic devices of increasing complexity. This is typically one of the most difficult problems to solve since it involves a large number of parameters, complex constraints, and objective functions with more than one optimum (Mescia et al., 2017). Moreover, in many cases, the optimization problem is non–linear and more challenging issues occur, especially when many local optimal solutions exist (Fornarelli et al., 2009; Yurtkuran, 2019).

Since the objective function is generally a multimodal one and considering that it is very difficult for deterministic algorithms to find the global optimal solution, many metaheuristic algorithms have become increasingly popular because of their potential in solving large-scale problems efficiently in a way that is impossible by using deterministic approaches. Compared to other nature-inspired optimization algorithms the swarm-inspired ones are gaining popularity within the electromagnetic research community and among electromagnetic engineers as design tool and problem solvers. In fact, they are able to efficiently find global optima without being trapped in local extrema as well as to address nonlinear and discontinuous problems characterized by great numbers of variables (Garg, 2014; Jin & Rahmat-Samii, 2007). However, according to the fact that there is no universal optimizer that can solve all optimization problems, a variety of swarm intelligence–based optimization algorithms have been developed. They include particle swarm optimization (PSO), ant colony optimization, cuckoo search, cockroach swarm optimization, firefly algorithm, bat algorithm, artificial fish swarm algorithm, flower pollination algorithm, artificial bee colony, wolf search algorithm, gray wolf optimization (Hassanien & Emary, 2016). As a result, the choice of a proper algorithm is a key issue especially considering that a general rule not exist, yet.

As in all swarm intelligence-based metaheuristic algorithms, the PSO is based on the general concept pertaining interaction and information exchange between multiple agents. In particular, it consists of population with members that locally interact each other following simple rules having some randomness. These interactions yield a collective intelligence resulting in a more organized and directive behavior than that of a stand alone individual. Since its introduction, PSO has received considerable attention by electromagnetic community as a powerful intelligent optimization method (Ciuprina et al., 2002; Jin & Rahmat-Samii, 2008; Robinson & Rahmat-Samii, 2004). The PSO paradigm has been successfully applied to solve different electromagnetic design problems because of its flexibility, efficiency, highly adaptability, implementation easiness, and many distinct features in different types of optimizations (Goudos et al., 2018; Greda et al., 2019; Mescia et al., 2011, 2014; Palma et al., 2014; Rehman et al., 2019; Xu & Fu, 2020). The PSO scheme provides better results in a faster and cheaper way with fewer parameter adjustments. Moreover, because its gradient–free mechanism the PSO is able to manage

very complex fitness functions with a limited number of control parameters. Due to the stochastic behavior, the classical PSO algorithms should need a lot of iterations to get a meaningful result. However, the current research on PSO has shown that it is easily trapped into local optima looking for the global optimum of difficult optimization problems. Thus, to overcome the unnecessary computational load, current research activities are focused on the refinements of the methods to create a good balance between precision, reliability and computational loads. In this regard, quantum inspired PSO was proposed to address such limitations and, in general, for treating a class of problems encountered in electromagnetic engineering (Fahad et al., 2021; Sun et al., 2011). A variant of QPSO was successfully developed to perform a systematic and detailed study of a new class of dielectric lens antennas (Bia et al., 2015; Mescia et al., 2016). A modified quantum inspired particle swarm optimizer was proposed for global optimization in the study of electromagnetic design problems (Rehman et al., 2019). An extended version of QPSO was coupled with fractional calculus-based FDTD algorithm to study the propagation of the electromagnetic waves inside arbitrary dispersive dielectric materials (Caratelli et al., 2016; Piro et al., 2016). Moreover, modified QPSO algorithms was proposed for global optimizations of electromagnetic inverse problems (Bia et al., 2016; Mescia et al., 2017; Rehman et al., 2018).

In many areas of electromagnetism, and in particular when analyzing antenna systems, it is of great importance to have a simple lumped–constant equivalent circuit to model the terminal behavior and receiving properties of radiating structures over a broad frequency range. In fact, it can provide computational convenience and physical insights into the operation and design of a broadband antenna. Moreover, the equivalent circuit would be useful to perform circuit simulations involving mixed frequency and time domains as well as simulations of antenna systems including nonlinear devices (Huang et al., 2021; Kim & Ling, 2005). As it is well known, a simple equivalent circuit can be used to model the driving-point antenna properties in narrow bands of frequencies around its resonance region. On the other hand, it is not easy to devise an equivalent circuit containing frequency dependent elements able to provide a broadband representation of the driving-point impedance function. Because of these modeling challenges, in this paper we describes an effective methodology pertaining the synthesis of broadband equivalent circuits with frequency and time invariant elements. Our task was to synthesize an equivalent circuit consisting of a finite number of lumped and linear elements, whose behavior at the feed terminals is a good approximation of the broadband frequency domain data concerning antenna simulations. To this aim, a quantum–inspired version of the PSO algorithm, namely the enhanced weighted quantum PSO (EWQPSO) has been specifically adopted to estimate and to optimize the equivalent circuit parameters for the best impedance fidelity. In this regard, our algorithm was tested considering the driving-point impedance calculated using the full–wave simulations of a conventional sinuous antenna in the frequency range from 1 to 3 GHz.

2. Methodology

This section provides a mathematical model of the social interactions of swarms, including conventional, quantum inspired and the proposed EWQPSO algorithm. The main issues regarding the problem of the network synthesis having a driving-point impedance/admittance function equal to a specified transcendental one are illustrated, too. Moreover, the Brune, Miyata, Butt and Duffin synthesis procedures are briefly outlined.

2.1. Optimization Algorithm

To better understand the proposed particle swarm methodology, a brief introduction on how conventional PSO works is given.

PSO is a swarm intelligence algorithm that mimic the social behavior of a swarm of bees or a flock of birds (Hassanien & Emary, 2016; Kennedy & Eberhart, 1995). If M denotes the swarm size and N the dimensionality of the search space, each individual i, $1 \le i \le M$, called particle, is initialized with random position $x_i = (x_{i1}, x_{i2}, \ldots, x_{iN})$ and velocity $v_i = (v_{i1}, v_{i2}, \ldots, v_{iN})$. Each particle adjusts its trajectory in the N-dimensional search space keeping track of the location corresponding to its best fitness value, called personal best, as well as the location corresponding to the best fitness value found by the whole swarm, called global best. In particular, the velocity v_{in} and position x_{in} of each particle are updated according to the following equations.

$$v_{in}(t+1) = w v_{in}(t) + c_1 r_1 \left[x_{in}^b(t) - x_{in}(t)\right] + c_2 r_2 \left[G_n(t) - x_{in}(t)\right] \quad (1)$$

$$x_{in}(t+1) = x_{in}(t) + v_{in}(t+1) \tag{2}$$

where $1 \leq n \leq N$ identifies the parameter to be optimized, t is the iteration counter, x_{in}^{b} and G_n are the personal and global best positions, respectively. The inertia weight w controls the current particle movement as well as the algorithm convergence. Large values of w improve exploration, while smaller values result in a confinement within an area surrounding the global maximum. r_1 and r_2 are two random positive numbers uniformly distributed in the range [0, 1], c_1 and c_2 are two positive constants, known respectively as cognitive and social parameter, which determine the convergence speed of the particles to x_{in}^{b} and G_n. At each next iteration, the x_{in}^{b} and G_n have to be updated with the current position and velocity minimizing the fitness function f. In particular, the personal best position of each particle is updated using the equation

$$x_{in}^{b}(t+1) = \begin{cases} x_{in}^{b}(t) & \text{if } f\left[x_{in}(t+1)\right] \geq f\left[x_{in}(t)\right] \\ x_{in}(t+1) & \text{if } f\left[x_{in}(t+1)\right] < f\left[x_{in}(t)\right] \end{cases} \tag{3}$$

and the global best position is defined as

$$G_n(t+1) = \operatorname{argmin} f\left[x_{in}^{b}(t+1)\right] \tag{4}$$

The PSO search performance may be degraded from stagnation and convergence to local minima since an improper balance between the local and global searches can occur. In fact, the particles located close to the local optimum solution could became inactive since their velocities could get close to zero. As a result, the PSO algorithm would be trapped in an undesired state of slow evolution. Such limitation becomes more restrictive when PSO is applied to complex electromagnetic problems characterized by large search spaces and multiple local optima. Moreover, the convergence speed is an important aspect to assess in these problems since the numerical evaluation of the fitness function generally takes a considerable amount of time. To solve such difficulties, the quantum–behaved particle swarm optimization algorithm was proposed (Sun et al., 2004). This algorithm permits all particles to move under the principles of quantum mechanics instead of the classical Newtonian dynamics imposed in PSO. In this way, the information about the velocity of the particles is no longer used as well as a good balance between local and global searches can be obtained. As a result, QPSO has a reduced number of control parameters, this making it easier to implement with a faster convergence rate, as well as it has a stronger search ability when applied to complex electromagnetic problems.

In the QPSO, the state of a particle is identified by the wave function, which is a solution of the Schrödinger equation instead of position and velocity. In this way, the exact values of x_{in} and v_{in} cannot be determined simultaneously, and it is only possible to learn the probability of the particle appearing in position x_{in} from probability density function. In particular, assuming that each particle move in the search space with a δ potential on each dimension, its movement is modeled according to the following iterative equation

$$x_{in}(t+1) = \begin{cases} p_{in}(t) + \dfrac{L_{in}(t)}{2} \ln\left(\dfrac{1}{u_{in}}\right) & \text{if } s_{in} \geq 0.5 \\ p_{in}(t) - \dfrac{L_{in}(t)}{2} \ln\left(\dfrac{1}{u_{in}}\right) & \text{if } s_{in} < 0.5 \end{cases} \tag{5}$$

where the location p_{in} of the potential energy distribution is given by

$$p_{in}(t) = \xi_{in}(t) x_{in}^{b}(t) + \left[1 - \xi_{in}(t)\right] G_n(t) \tag{6}$$

and the standard deviation of the distribution L_{in} can be calculated as

$$L_{in}(t) = 2\beta \left| \bar{x}_n(t) - x_{in}(t) \right| \tag{7}$$

In Equations 5 and 6 u_{in}, s_{in} and ξ_{in} are random numbers uniformly distributed in [0, 1], respectively. The number u_{in} results from the process of collapsing the quantum state to the classical one. The ξ_{in} parameter quantifies the probability of the $i-th$ particle appearing in its personal best position (Cai et al., 2008). Moreover, s_{in} results

from the employment of the Monte Carlo inverse method to obtain the position function. The mean best position $\bar{x}_n$, that is the mean of the personal best positions of all particles, is given by

$$\bar{x}_n(t) = \frac{1}{M}\sum_{i=1}^{M} x_{in}^{b}(t) \tag{8}$$

The parameter β is called contraction–expansion coefficient. In particular, considering that the number of iteration and the population size are common requirements, it is the only parameter that can be tuned to control the convergence speed of the QPSO algorithm.

By an inspection of Equation 8 it is clear that each particle affects in the same way the mean of the personal best positions. In this way, each particle has equal importance compared to the others and in some cases the corresponding searching approach can be reasonable. On the other hand, based on general rules of real-life social culture, the equally weighted mean position could represent not the best choice since some particles can have a greater importance than others. To this aim, a control method based on the promotion of the particle importance has been developed (Xi et al., 2008). In such approach, the particle has a weighted coefficient linearly decreasing with the corresponding fitness function. The closer is the fitness function to the optimal value, the larger is the weight of the particle. As a result, the best position can be calculated as

$$\bar{x}_n(t) = \frac{1}{M}\sum_{i=1}^{M} \alpha_i x_{in}^{b}(t) \tag{9}$$

where the weighting coefficient α_i linearly ranges from 1.5, for the best particle, down to 0.5 for the worst one (Xi et al., 2008). The resulting algorithm is called Weighted Quantum-Behaved Particle Swarm Optimization (WQPSO) and it shows a better convergence efficiency than the QPSO.

The convergence speed is important in electromagnetic problems since every run of the objective function takes a considerable amount of time. As a result, any effort to reduce the computational time characterizing the whole optimization process is much relevant. Within this framework, and, in particular, to further improve the convergence rate of the WQPSO algorithm, we have developed an enhanced weighting methodology where the computation of the mean best position is carried out by directly embedding the information associated with the error function. The resulting EWQPSO algorithm is based on the following adaptive update equation:

$$\bar{x}_n(t) = \frac{\sum_{i=1}^{M} \Delta_i(t) x_{in}^{b}(t)}{\sum_{i=1}^{M} \Delta_i(t)} \tag{10}$$

where

$$\Delta_i(t) = \begin{cases} 1 - \dfrac{\mathcal{E}\left[\mathbf{P}_i(t)\right]}{\max\left\{\mathcal{E}\left[\mathbf{P}_1(t)\right], \mathcal{E}\left[\mathbf{P}_2(t)\right], \ldots, \mathcal{E}\left[\mathbf{P}_M(t)\right]\right\}} & \text{Minimization problem} \\ 1 - \dfrac{\min\left\{\mathcal{E}\left[\mathbf{P}_1(t)\right], \mathcal{E}\left[\mathbf{P}_2(t)\right], \ldots, \mathcal{E}\left[\mathbf{P}_M(t)\right]\right\}}{\mathcal{E}\left[\mathbf{P}_i(t)\right]} & \text{Maximization problem} \end{cases} \tag{11}$$

$\mathcal{E}$ is the error function and $\mathbf{P}_i(t) = \left[x_{i1}^{b}(t), x_{i2}^{b}(t), \ldots, x_{iN}^{b}(t)\right]$. In this way, the particles close to the optimum value will stochastically guide the movements of the whole swarm. Moreover, the absorbing boundary condition has been implemented and, in particular, every particle which flies outside the search range in one specific dimension is going to be moved back at the boundary of the search range along that dimension (El-Abd & Kamel, 2007; Mescia et al., 2017; Xi et al., 2008).

2.2. Equivalent Circuit Model

Generally, the impedance/admittance of an electromagnetic structures having distributed constant, such as for example antennas, can be exactly represented at all frequencies by transcendental functions satisfying specific conditions. So, with reference to the problem of the network synthesis, it is useful to determine a network

comprising lumps of constant resistance, inductance, conductance and capacitance whose driving–point impedance/admittance function is equal to the specified transcendental one at all frequencies (real and complex). A way to solve this problem is based on a well-known proposition of function theory providing a tool for breaking up a transcendental function into an infinite series of simple fractions. The resulting series representation provides a means of determining the network having in general an infinite number of branches (Pearson & Wilton, 1981; Streable & Pearson, 1981). However, in order to ensure that the function is the impedance/admittance of a physically realizable linear and passive electric circuit structure it has to be a positive real function (PRF) satisfying the following restrictions:

1. the structure shall be stable or equivalently every natural mode of oscillation dies away exponentially;
2. the natural oscillations are real function of the time;
3. if a sinusoidal current flows at the driving–point terminals of the equivalent structure, the average real power delivered to it will be positive

Let $Y(s)$ be the complex function, modeling the driving–point admittance and $s = \sigma + j\omega$ the independent complex variable. Let $p_1, p_2, \ldots$ be the poles of $Y(s)$, except for the point at infinity which is an essentially singular point, and $A_1, A_2, \ldots$ be the residues at the poles where

$$0 < |p_1| \leq |p_2| \leq |p_3| \leq \cdots \leq |p_n| \quad n \to \infty \tag{12}$$

Then the following series development for $Y(s)$ can be given (Streable & Pearson, 1981):

$$Y(s) = \lim_{N\to\infty} \sum_{n=-N}^{N} \left(\frac{A_n}{s - p_n} + \frac{A_n}{p_n} \right) \tag{13}$$

where, by virtue of restriction 2, the terms in the series (13) occur in pairs with conjugate complex poles and residues, that is, $p_{-n} = p_n^*$ and $A_{-n} = A_n^*$. The network will contain an infinite number of branches connected in parallel each one representing the pairs of terms, although a finite number may be used if it is desired to represent only specific modes. This truncation has to be done in a such way to maintain the PRF characteristics. However, if the admittance of all the branches are PRF any finite sum of admittance terms will be a PRF. Synthesis techniques for obtaining a network representation for a rational function, such as the one comprising a pair of terms in the series (13), are well known.

By using the Brune synthesis, every PRF can be realized as the driving-point impedance of an RLC circuit. The poles and zeros of the PRF can be anywhere in the left half of the complex plane. It is a canonical realization characterized by a number of lumped elements equal to the number of coefficients of the impedance function (Wing, 2008). The Brune synthesis can be only applied to minimum-reactance and minimum-susceptance function. So, it requires a series of preliminary steps aimed to remove any and all poles and zeros on the $j\omega$ axis, including the point $s = 0$ and $s = \infty$. Anyway, the Brune synthesis generates a ladder network containing an undesirable element appearing either as a perfectly coupled transformer or a negative inductance. Neither of these elements is realizable without the use of active device. Miyata method eliminates the need of ideal transformers. It is based on the split of the real part of a given minimum reactive driving point impedance into a sum of even function. This synthesis is used for the real part of an impedance with all non-negative coefficients. If there are negative coefficients, it introduces surplus factors (Miyata, 1955). However, even if the Miyata synthesis procedure is more practical its implementation is more complicated because no single format of the synthesis is applicable to a general PRF (Wing, 2008). Moreover, an inherent difficulty lies in the requirement that the additive components have to be positive for each angular frequency. The Bott-Duffin method is another general procedure to synthesize a PRF as the impedance/admittance of a circuit composed of only resistors, capacitors and inductors, without transformers (Wing, 2008). For some PRF, the networks obtained by applying this procedure are minimal both in number of reactive elements and resistors among series-parallel networks (Hughes & Smith, 2014). Moreover, the Bott-Duffin procedure, in combination with some simple network transformations, can be used to produce all of the series-parallel networks containing exactly six reactive elements and two resistors which realize any specified biquadratic minimum function. Due to these features and its capabilities to the automated implementation, the Butt -Duffin method has been used in this work. Thus the equivalent circuit resulting from application of this procedure is given in Figure 1.

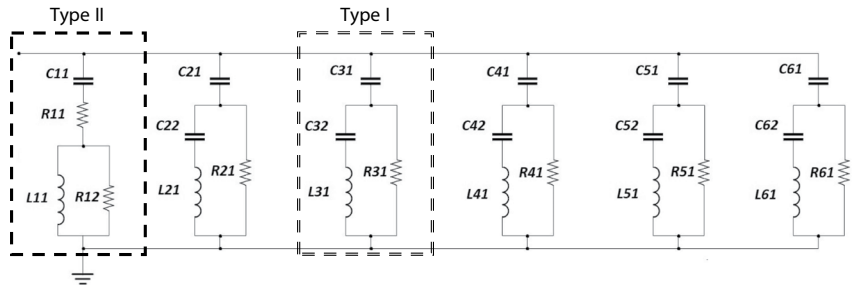

Figure 1. Equivalent circuit based on Bott–Duffin realization.

3. Numerical Results

3.1. Mathematical Test

In order to test the performance of the proposed EWQPSO in terms of convergence rate, precision, and robustness five benchmark functions, as tabulated in Table 1, were considered (Jamil & Yang, 2013; Neculai, 2008). We choose these functions because they provide a balance of uni-modal and multi-modal behavior as well as their non-linearity and many local minima around the global minimum point. Moreover, for all these functions the global minimum is $f(x) = 0$ placed at $x = (0, \ldots, 0)$.

The Ipersphere function is the simplest one and it is continuous, convex and unimodal. The Alpine function is non-convex, non-continuous, differentiable and separable. The modified fourth De Jong function exhibits the global minimum in a narrow parabolic valley. However, even if this valley is easy to find, the convergence to the minimum is difficult. The Zakharov function is a representative of the plate–shaped functions. It has no local minima except the global one. The Salomon function is continuous, differentiable, non–separable, scalable and multimodal. The minimum searching problem regarding the considered test functions is considered by changing both the domain dimension N and the swarm size M. The maximum generation value is set to $t_{\max} = 500 + 10N$. The performance of the EWQPSO algorithm was then compared with those of QPSO and WQPSO in terms of global standard deviation and mean value by considering 100 independent runs. The considered fitness function is the root mean square error.

A number of investigations were performed by changing the number of particles $N = 5$, 10, 15, 20 and the contraction–expansion coefficient in the range from 0.5 to 50. This investigation was carried out with the aim of analyzing the effect of these free parameters on the searching capabilities of the optimization algorithm in terms of accuracy and convergence speed. The obtained results are summarized in Table 2. The outcomes of Table 2 reveal that the developed EWQPSO algorithm is characterized by improved global searching capability as well as better performance in terms of convergence and accuracy as compared to standard QPSO and WQPSO. In fact, by an inspection of the obtained numerical results it can be inferred that for each test function the proposed EWQPSO finds the global minimum with an accuracy at least 10^5 times better than the QPSO and WQPSO. In the case of the Alpine function, the EWQPSO exhibits the better performance providing a value of 1.48×10^{-12} that is about 10^7 times less than that found by QPSO and WQPSO. In addition, the variance values obtained by the EWQPSO algorithm are the smallest. This result confirms the enhanced searching ability of the EWQPSO. Figure 2 shows the convergence plots of the different optimization algorithms for each test function. In particular, the best objective function value, in a logarithmic scale, is reported using a domain dimension $N = 20$ and a population of $M = 30$ particles. The performed analysis illustrates that the proposed EWQPSO, in addition to search the optimal solution with better accuracy, is characterized by a faster convergence speed since it requires a lower number of iterations to find the minimum. In fact, for all the test functions the plot corresponding to the EWQPSO is always below the others. As an example, in the case of the Alpine function the EWQPSO finds the minimum value of about 10^{-4} with about 500 fewer iterations then those used by the WQPSO.

Table 1
Test Functions

Function name	Expression	Input domain
Ipersphere	$f(x) = \sum_{i=1}^{N} x_i^2$	$x_i \in [-100, 100]$
Alpine	$f(x) = \sum_{i=1}^{N} \lvert x_i \sin(x_i) + 0.1x_i \rvert$	$x_i \in [-10, 10]$
De Jong	$f(x) = \sum_{i=1}^{N} i x_i^4$	$x_i \in [-100, 100]$
Zakharov	$f(x) = \sum_{i=1}^{N} x_i^2 + \left(\sum_{i=1}^{N} 0.5 i x_i\right)^2 + \left(\sum_{i=1}^{N} 0.5 i x_i\right)^4$	$x_i \in [-10, 10]$
Salomon	$f(x) = 1 - \cos\left(2\pi\sqrt{\sum_{i=1}^{N} x_i^2}\right) + 0.1\sqrt{\sum_{i=1}^{N} x_i^2}$	$x_i \in [-100; 100]$

Table 2
Performance Comparison of EWQPSO, QPSO and WQPSO Algorithms

		QPSO		WQPSO		EWQPSO	
Function	N	Mean	std	Mean	std	Mean	std
Sphere	5	6.79×10^{-94}	6.74×10^{-93}	2.28×10^{-93}	2.11×10^{-92}	6.35×10^{-110}	3.66×10^{-109}
	10	9.80×10^{-88}	5.67×10^{-87}	3.77×10^{-86}	2.99×10^{-85}	5.93×10^{-98}	1.84×10^{-97}
	15	3.22×10^{-77}	1.18×10^{-76}	8.24×10^{-76}	3.64×10^{-75}	3.72×10^{-83}	3.03×10^{-82}
	20	9.74×10^{-67}	5.75×10^{-66}	1.57×10^{-65}	1.14×10^{-64}	1.43×10^{-71}	4.09×10^{-71}
Alpine	5	5.04×10^{-5}	1.39×10^{-4}	5.76×10^{-5}	1.70×10^{-4}	2.24×10^{-6}	1.71×10^{-5}
	10	6.42×10^{-5}	3.60×10^{-4}	2.76×10^{-5}	1.34×10^{-4}	5.26×10^{-7}	5.15×10^{-6}
	15	6.24×10^{-7}	5.10×10^{-6}	1.67×10^{-4}	1.56×10^{-3}	1.07×10^{-4}	1.07×10^{-3}
	20	2.63×10^{-5}	2.20×10^{-4}	3.29×10^{-4}	2.32×10^{-3}	1.48×10^{-12}	1.34×10^{-11}
De Jong	5	1.21×10^{-175}	0	1.48×10^{-172}	0	7.69×10^{-202}	0
	10	2.85×10^{-144}	2.85×10^{-143}	1.63×10^{-144}	1.10×10^{-141}	4.58×10^{-158}	4.06×10^{-157}
	15	5.44×10^{-118}	3.12×10^{-117}	4.17×10^{-117}	2.47×10^{-116}	2.52×10^{-123}	1.76×10^{-122}
	20	6.02×10^{-95}	3.05×10^{-94}	1.42×10^{-92}	1.09×10^{-91}	8.80×10^{-99}	3.77×10^{-98}
Zakharov	5	5.30×10^{-7}	5.28×10^{-6}	8.02×10^{-10}	4.96×10^{-9}	8.60×10^{-14}	3.63×10^{-13}
	10	5.24×10^{-7}	1.55×10^{-6}	7.26×10^{-6}	6.95×10^{-5}	1.65×10^{-9}	9.22×10^{-9}
	15	1.43×10^{-4}	9.30×10^{-4}	1.60×10^{-5}	1.02×10^{-4}	8.20×10^{-8}	2.11×10^{-7}
	20	5.02×10^{-4}	1.68×10^{-3}	2.77×10^{-4}	1.09×10^{-3}	5.98×10^{-6}	2.07×10^{-5}
Salomon	5	9.41×10^{-52}	3.69×10^{-51}	5.04×10^{-51}	2.26×10^{-50}	1.63×10^{-61}	9.50×10^{-61}
	10	1.19×10^{-49}	3.42×10^{-49}	9.12×10^{-49}	1.92×10^{-48}	3.28×10^{-57}	5.91×10^{-57}
	15	2.28×10^{-45}	3.08×10^{-45}	2.10×10^{-44}	4.39×10^{-44}	2.47×10^{-51}	3.97×10^{-51}
	20	1.13×10^{-40}	1.52×10^{-40}	4.02×10^{-39}	2.98×10^{-38}	1.88×10^{-45}	3.33×10^{-45}

3.2. Equivalent Circuit Synthesis

After the preliminary analysis aimed to demonstrate that the EWQPSO can efficiently extend the solution quality and convergence behavior of the QPSO, the developed optimization algorithm has been used to evaluate the lumped element values characterizing the equivalent circuit whose driving–point admittance function well approximate the antenna admittance calculated using the Ansys Electronic Suite (Ansys Electronics, n.d.). To this aim, a two arms sinuous antenna printed on a RT/duroid®5880 laminate was simulated in the frequency range 1–3 GHz (DuHamel, 1987; Mescia et al., 2022). Other parameters characterizing the antenna are the number of cells $p = 12$, the angular width $\alpha = \pi/2$, the angular spacing $\delta = \pi/4$, the grow rate $\tau = 0.78$, and the radius of the outermost cell $R = 29$ mm. Figure 3 illustrates the sketch of the antenna and Figure 4 (see blue curve) shows the real and imaginary part spectrum of the driving–point admittance $\tilde{Y}$, calculated using the electromagnetic tool. By an inspection of the plot pertaining the real part of $\tilde{Y}$, five resonances (two well resolved and three overlapped) can be identified. As a result, the equivalent circuit illustrated in Figure 1 can be inferred. The type II four element circuit is selected to match the antenna admittance in the highest part of the spectrum. On the other hand, the five circuits of type I are used to model the antenna resonances when the operating frequency increases.

The developed EWQPSO algorithm is employed with the aim to obtain values of parameters minimizing a specific fitness function. In particular, the algorithm is performed by setting a swarm composed by $M = 1200$ particles, whose position vector of the $i - th$ particle consists of $N = 24$ elements, each one corresponding to a lumped element characterizing the equivalent circuit illustrated in Figure 1. The maximum number of iteration was fixed to $t = 10^4$, whereas the fitness function was computed by considering the deviation of the values yielded by the EWQPSO from those calculated using the electromagnetic tool. In particular, it was evaluated by considering the error function

$$\varepsilon_j = \frac{1}{L}\sqrt{\sum_{l=1}^{L}\left(Y_{lj} - \tilde{Y}_l\right)^2} \tag{14}$$

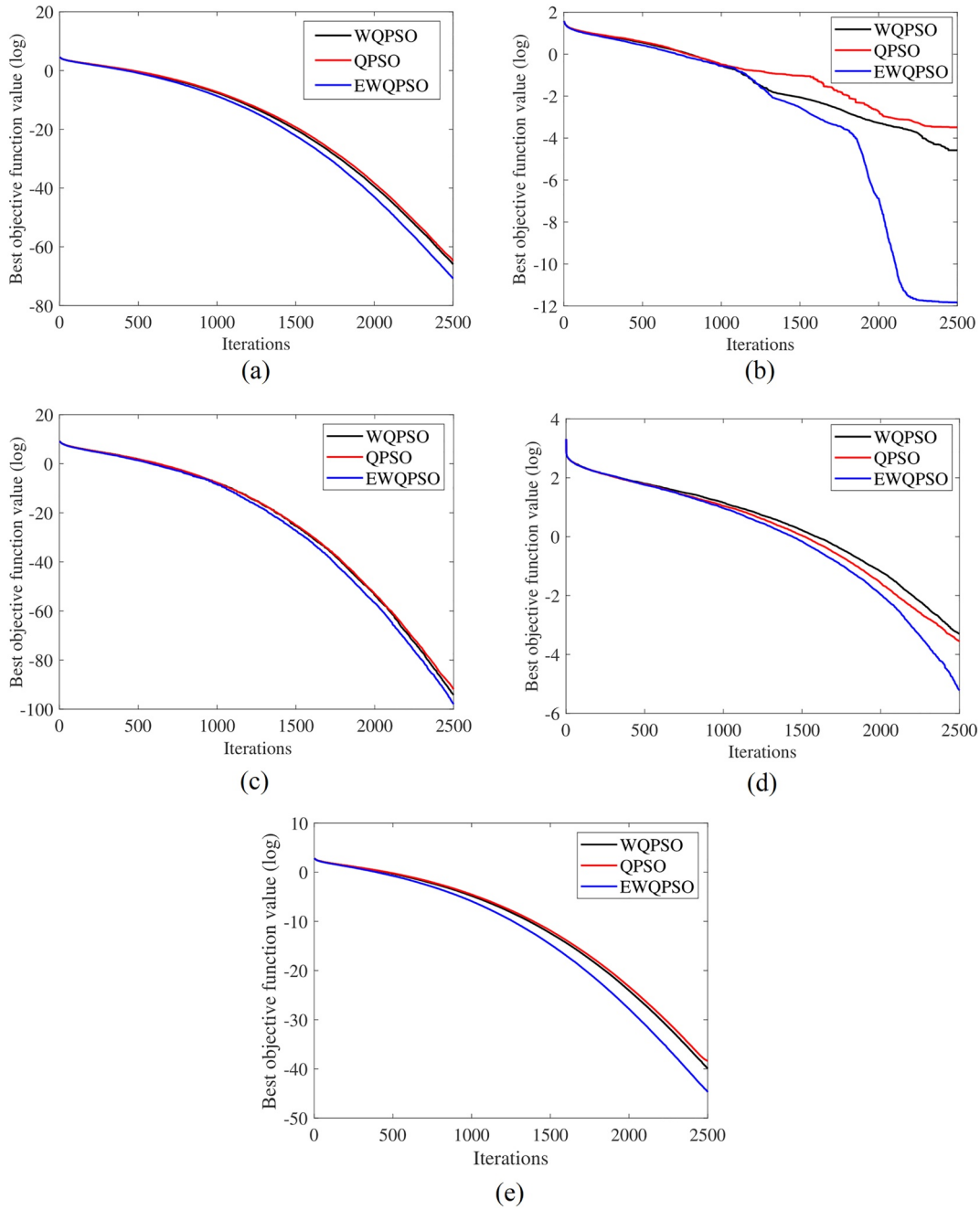

Figure 2. Comparison of the convergence plots. (a) Ipersphere, (b) Alpine, (c) De Jong, (d) Zakharov, (e) Salomon test functions.

where L is the number of points the entire frequency range has been sampled, Y_{lj} and $\tilde{Y}_l$ are the driving–point admittances of the equivalent circuit illustrated in Figure 1 calculated using EWQPSO and Ansys Electronic Suite, respectively. In Equation 14, j and l correspond to the particle and frequency sample, respectively.

The search range of the variable corresponding to the lumped circuit element was roughly fixed such that the minimum of the fitness function is expected. First, a narrow band model based on bandwidths, center frequency or resonant frequencies of antenna is used to roughly estimate the component values. With reference to the RLC tanks indicated as Type I, the series capacitor value was selected to match the antenna reactance at a frequency much lower than the resonant one. Thus, the effect of the parallel resonant RLC network may be ignored. On

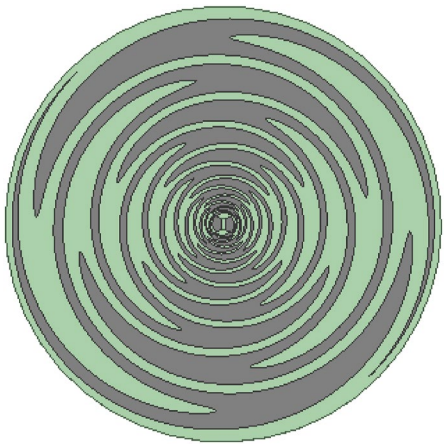

Figure 3. Sketch of the sinuous antenna with radius $R = 29$ mm, $\alpha = \pi/2$, $\delta = \pi/4$ and $\tau = 0.78$.

the other hand, the component values of the RLC circuit are estimated at the resonant frequency at which the reactance of the antenna vanishes. This estimation is useful for evaluating the search range of each particle in such a way the EWQPSO algorithm can find the optimal values of the lumped elements. After all parameters characterizing the admittance function were estimated, a local adjustment of the component values was made using EWQPSO to ensure the best fit of the input admittance with that of the antenna around each resonant frequency.

This preliminary investigation only serves as an approximation for the modeling of driving–point admittance. In fact, for frequencies higher than 1.8 GHz the antenna exhibited a challenging behavior characterized by three strongly overlapped resonances (see Figure 4). As a result, it is essential a further adjustment of all the lumped element values to increase the accuracy of input admittance matching over the whole frequency range. In order to support this claim, in Figure 5 are plotted the admittance of each branch forming the equivalent circuit reported in Figure 1, and the whole driving-point admittance (black curve). All the curves were obtained using the narrow band model and the local EWQPSO adjustment. The red curve is the same reported in Figure 4. By an inspection of Figure 5 it can be observed that the real and imaginary parts of the driving-point admittance, in the highest part of the spectrum, practically coincide with those of the type II RLC circuit. On the other hand, it has a negligible effect on the driving-point admittance in the lowest part of the spectrum. However, due to its fairly broadband admittance, the type II circuit is also used to improve the admittance matching at intermediate frequencies. As expected, a discrepancy between the optimal and narrow band admittance can be detected in the highest part of the spectrum. So, to improve the accuracy of the equivalent circuit synthesis procedure the EWQPSO was executed again with the aim to perform a global optimization of all the component values minimizing the error function over the whole frequency range. Once the best results were obtained, the mean and standard deviation of the lumped elements characterizing the equivalent circuit were calculated by considering 100 independent runs of the EWQPSO algorithm. The obtained results are summarized in Table 3. Moreover, in Figure 4 are reported the real and imaginary part of the driving-point admittance corresponding to the mean values of the lumped elements. It is worthwhile to note the very good agreement between both real part (see Figure 4a) and imaginary part (see Figure 4b) of the admittance calculated using the electromagnetic tool (blue curve in Figure 4) and the one recovered using the developed EWQPSO algorithm (red curve in Figure 4).

The contraction-expansion coefficient β influences the exploration searching ability of the particles. A large value of β result in greater population diversity making possible a more global search of the EWQPSO algorithm

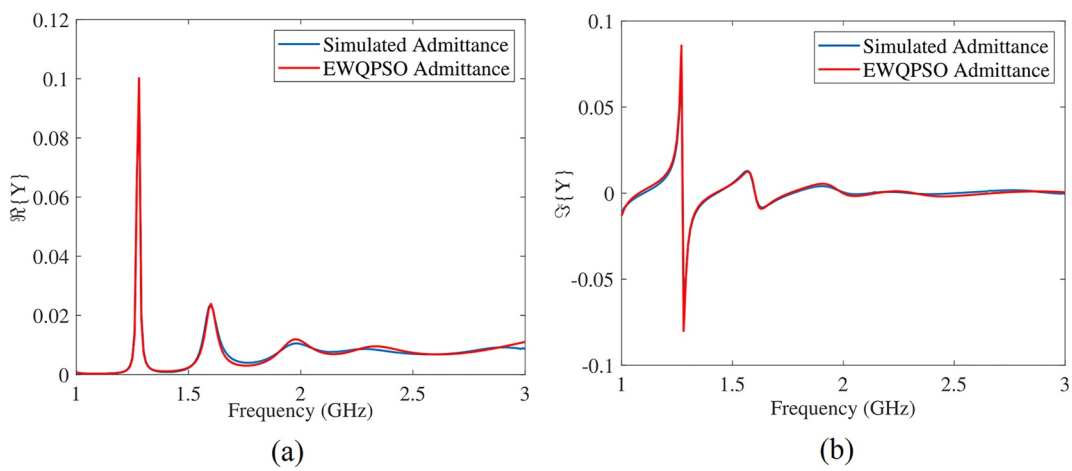

Figure 4. (a) Real and (b) imaginary part of the driving-point admittance versus the frequency evaluated using both the electromagnetic tool (blue curve) and enhanced weighted quantum particles swarm optimization (EWQPSO) algorithm (red curve).

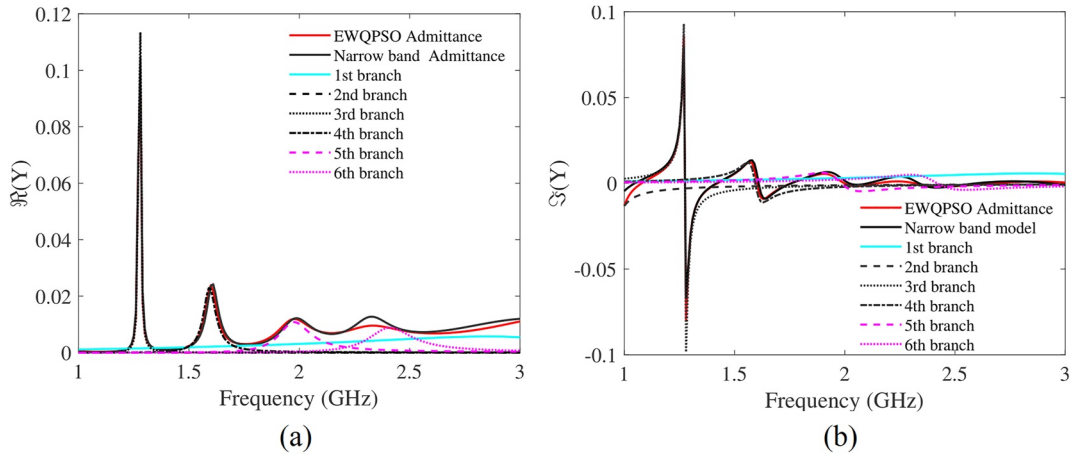

Figure 5. Driving-point admittance spectrum (black curve) and admittance spectrum of each branch calculated using the narrow band model and the local enhanced weighted quantum particles swarm optimization (EWQPSO) adjustment. Optimal driving-point admittance spectrum (red curve). (a) Real part and (b) imaginary part.

(global exploration). On the other hand, lower values of β cause a more focused exploration of the search space (local exploration). Suitable selection of β can provide a balance between global and local exploration ability and thus save the iterations number to find the optimum. In order to investigate this important issue, a number of simulations changing the contraction-expansion coefficient were carried out. Figure 6 shows the maximum, minimum and mean error characterizing the whole swarm versus the iteration time and for $\beta = 0.5$, $\beta = 10$ and $\beta = 50$. By an inspection of the obtained results, it is clear that the searching capabilities of the whole swarm improves as β increases. In fact, in contrast to $\beta = 0.5$ and $\beta = 5$, when $\beta = 50$ the maximum, minimum and mean errors converge to the same value, thus confirming that almost all the particles find the same optimal solution. It can be also observed that the calculation method with $\beta = 50$ can make the convergence speed of EWQPSO faster. In this case, the EWQPSO needs of about 700 iterations to reach the minimum error value of 10^{-4}, which is about half the number of iterations required by the algorithm having $\beta = 0.5$. Finally, it can be inferred that the EWQPSO with $\beta = 50$ exhibits better global search capabilities in comparison to EWQPSO with $\beta = 0.5$ and $\beta = 5$ as well as it provides a better optimal result.

4. Conclusions

A modified QPSO-based method for solving complicated electromagnetic optimization problems was illustrated. The applicability of the EWQPSO was investigated with the aim to synthesize the lumped element circuit of the feed–point antenna impedance. The proposed approach was first compared with both the standard and weighted QPSO. The outcomes on standard test functions highlight that the EWQPSO method has better global searching capability and faster convergence speed. The optimization problem was formulated with the aim of improving the fit between the input admittance of the equivalent circuit and the feed–point antenna admittance calculated using

Table 3
Mean and Standard Deviation Values Pertaining the Lumped Elements of the Equivalent Circuit Reported in Figure 1

	C_{r1}(pF)		C_{r2}(pF)		R_{r1}(kΩ)		R_{12}(Ω)		L_{r1}(nH)	
branch	Mean	std	Mean	std	Mean	std	Mean	std	Mean	std
1st	0.2	4.33×10^{-9}	–	–	1.62	4.22×10^{-15}	49.8	4.83×10^{-14}	11.87	3.11×10^{-14}
2nd	1.03	3.75×10^{-15}	0.87	2.95×10^{-15}	68.88	6.84×10^{-13}	–	–	63.14	2.39×10^{-13}
3rd	0.23	1.43×10^{-8}	0.47	1.43×10^{-8}	44.47	2.32×10^{-9}	–	–	102.07	8.71×10^{-12}
4th	0.08	2.57×10^{-13}	9.33	2.08×10^{-8}	35.84	3.38×10^{-10}	–	–	125.40	4.87×10^{-6}
5th	0.08	1.8×10^{-16}	2.52	2.22×10^{-13}	10	3.38×10^{-10}	–	–	84.5	4.02×10^{-7}
6th	0.07	1.66×10^{-14}	0.6	2.99×10^{-15}	6	1×10^{-14}	–	–	75	2.57×10^{-13}

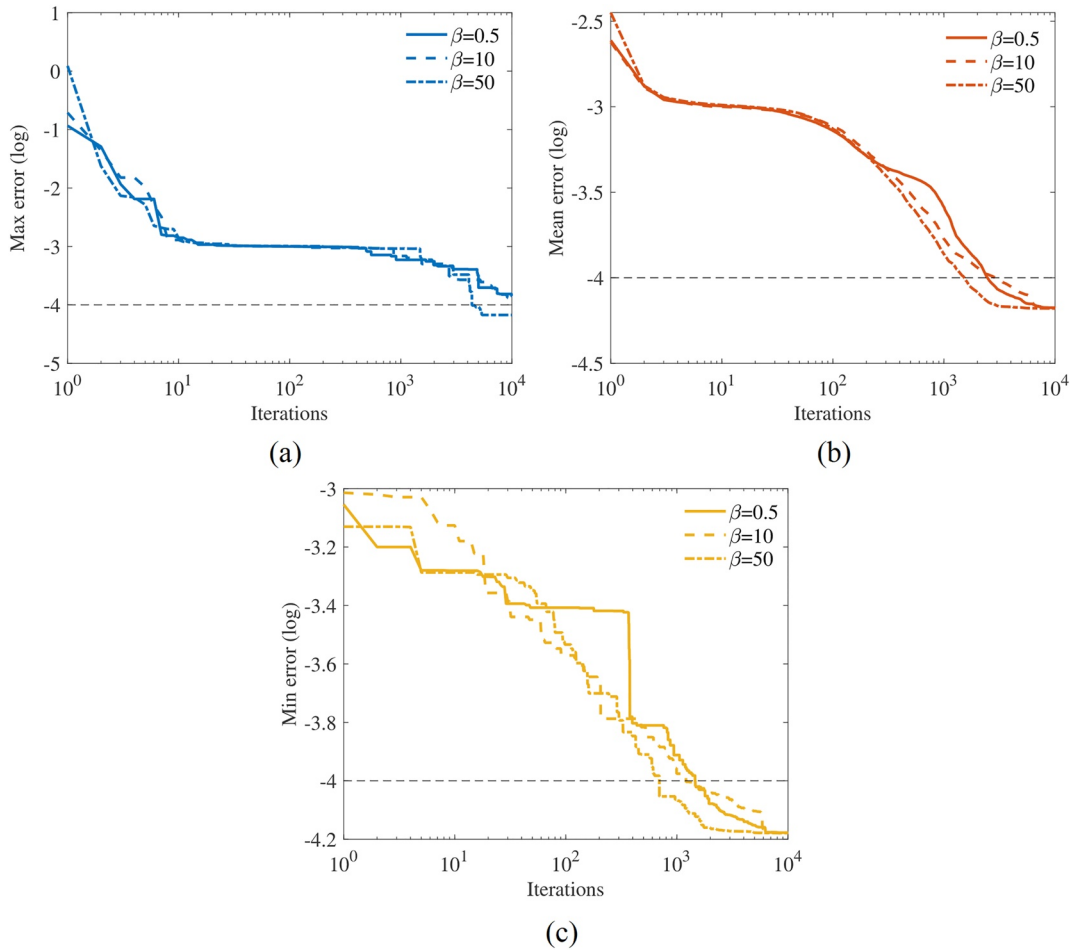

Figure 6. (a) Maximum, (b) minimum and (c) mean error versus the iteration time.

and electromagnetic tool in a specific frequency range. The values of the lumped elements forming the equivalent circuit was considered as the design variables for EWQPSO numerical tool. Final results show a perfect match of the simulated admittance plot with the one resulting from the EWQPSO optimization, demonstrating the efficient use of the algorithm to synthesize equivalent circuits. Moreover, it was found that a contraction–expansion coefficient $\beta = 50$ guarantees the better balance between the global and local search abilities. The proposed approach allows an easy incorporation of any changes in design parameters without necessitating any major changes to current framework, making it robust, generic and flexible. As a result, the EWQPSO could be a favorable alternative for global optimization in the study of electromagnetic design problems.

Data Availability Statement

No data come from previously published sources, and all simulation results are obtained with the software Matlab Suite as well as Ansys Electronic Suite. The data are deposited in a public accessible domain and can be found in the link https://zenodo.org/record/6405941#.YkbrfChBxPY.

Acknowledgments
Open Access Funding provided by Politecnico di Bari within the CRUI-CARE Agreement.

References

Ansys Electronics. (n.d.). Retrieved from https://www.ansys.com/it-it/products/electronics

Bia, P., Caratelli, D., Mescia, L., & Gielis, J. (2015). Analysis and synthesis of supershaped dielectric lens antennas. *IET Microwaves, Antennas & Propagation*, *9*(14), 1497–1504. https://doi.org/10.1049/iet-map.2015.0091

Bia, P., Mescia, L., & Caratelli, D. (2016). Fractional calculus-based modeling of electromagnetic field propagation in arbitrary biological tissue. *Mathematical Problems in Engineering*, 1–11. ID 5676903. https://doi.org/10.1155/2016/5676903

Cai, Y., Sun, J., Wang, J., Ding, Y., Tian, N., Liao, X., & Xu, W. (2008). Optimizing the codon usage of synthetic gene with QPSO algorithm. *Journal of Theoretical Biology*, *254*(1), 123–127. https://doi.org/10.1016/j.jtbi.2008.05.010

Caratelli, D., Mescia, L., Bia, P., & Stukach, O. (2016). Fractional-calculus-based FDTD algorithm for ultrawideband electromagnetic characterization of arbitrary dispersive dielectric materials. *IEEE Transactions on Antennas &&; Propagation*, *64*(8), 3533–3544. https://doi.org/10.1109/tap.2016.2578322

Ciuprina, G., Ioan, D., & Munteanu, I. (2002). Use of intelligent-particle swarm optimization in electromagnetics. *IEEE Transactions on Magnetics*, *38*(2), 1037–1040. https://doi.org/10.1109/20.996266

DuHamel, R. H. (1987). Dual polarized sinuous antenna. *U.S. Patent*, *4*, 658–262.

El-Abd, M., & Kamel, M. (2007). Particle swarm optimization with varying bounds. In *IEEE Congress on Evolutionary Computation* (pp. 4757–4761).

Fahad, S., Yang, S., Khan, R., Khan, S., & Khan, S. (2021). A multimodal smart quantum particle swarm optimization for electromagnetic design optimization problems. *Energies*, *14*(15), 4613. https://doi.org/10.3390/en14154613

Fornarelli, G., Mescia, L., Prudenzano, F., Sario, M. D., & Vacca, F. (2009). A neural network model of erbium-doped photonic crystal fibre amplifiers. *Optics & Laser Technology*, *41*(5), 584–585. https://doi.org/10.1016/j.optlastec.2008.10.010

Garg, H. (2014). Solving structural engineering design optimization problems using an artificial bee colony algorithm. *Journal of Industrial and Management Optimization*, *10*(3), 777–794. https://doi.org/10.3934/jimo.2014.10.777

Goudos, S., Zaharis, Z., & Baltzis, K. (2018). Particle swarm optimization as applied to electromagnetic design problems. *International Journal of Swarm Intelligence Research*, *9*(2), 47–82. https://doi.org/10.4018/ijsir.2018040104

Greda, L., Winterstein, A., Lemes, D., & Heckler, M. (2019). Beamsteering and beamshaping using a linear antenna array based on particle swarm optimization. *IEEE Access*, *7*, 141562–141573. https://doi.org/10.1109/access.2019.2944471

Hassanien, A. E., & Emary, E. (2016). *Swarm intelligence principles, advances, and applications*. CRC Press.

Huang, Y., Alieldin, A., & Song, C. (2021). Equivalent circuits and analysis of a generalized antenna system. *IEEE Antennas and Propagation Magazine*, *63*(2), 53–62. https://doi.org/10.1109/map.2021.3053976

Hughes, T., & Smith, M. (2014). On the minimality and uniqueness of the Bott–Duffin realization procedure. *IEEE Transactions on Automatic Control*, *59*(7), 1858–1873. https://doi.org/10.1109/tac.2014.2312471

Jamil, M., & Yang, X.-S. (2013). A literature survey of benchmark functions for global optimisation problems. *IEEE Transactions on Antennas and Propagation*, *4*(2), 150–194. https://doi.org/10.1504/ijmmno.2013.055204

Jin, N., & Rahmat-Samii, Y. (2007). Advances in particle swarm optimization for antenna designs: Real-number, binary, single-objective and multiobjective implementations. *IEEE Transactions on Antennas and Propagation*, *55*(3), 556–567. https://doi.org/10.1109/tap.2007.891552

Jin, N., & Rahmat-Samii, Y. (2008). Particle swarm optimization for antenna designs in engineering electromagnetics. *Journal of Artificial Evolution and Applications*, *2008*, 728929. https://doi.org/10.1155/2008/728929

Kennedy, J., & Eberhart, R. (1995). Particle swarm optimization. In *Proceedings of IEEE International Conference on Neural Networks* (pp. 1942–1948).

Kim, Y., & Ling, H. (2005). Equivalent circuit modelling of broadband antennas using a rational function approximation. *Microwave and Optical Technology Letters*, *48*(5), 950–953. https://doi.org/10.1002/mop.21529

Mescia, L., Bia, P., Caratelli, D., Chiapperino, M., Stukach, O., & Gielis, J. (2016). Electromagnetic mathematical modeling of 3-D supershaped dielectric lens antennas. *Mathematical Problems in Engineering*, 1–10. ID 8130160. https://doi.org/10.1155/2016/8130160

Mescia, L., Bia, P., Caratelli, D., & Gielis, J. (2017). Swarm intelligence for electromagnetic problem solving. In *Soft Computing and Nature-Inspired Algorithms* (pp. 69–100). IGI Global.

Mescia, L., Giaquinto, A., Fornarelli, G., Acciani, G., sario, M. D., & Prudenzano, F. (2011). Particle swarm optimization for the design and characterization of silica-based photonic crystal fiber amplifiers. *Journal of Non-Crystalline Solids*, *357*(8–9), 1851–1855. https://doi.org/10.1016/j.jnoncrysol.2010.12.049

Mescia, L., Girard, S., Bia, P., Robin, T., Laurent, A., Prudenzano, F., et al. (2014). Optimization of the design of high power Er^{3+}/Yb^{3+}-codoped fiber amplifiers for space missions by means of particle swarm approach. *IEEE Journal of Selected Topics in Quantum Electronics*, *20*, 484–491. ID 3100108. https://doi.org/10.1109/jstqe.2014.2299635

Mescia, L., Mevoli, G., Lamacchia, C., Gallo, M., Bia, P., Gaetano, D., & Manna, A. (2022). Sinuous antenna for UWB radar applications. *Sensors*, *22*(1), 248. https://doi.org/10.3390/s22010248

Miyata, F. (1955). A new system of two-terminal synthesis. *IRE Transactions on Circuit Theory*, *2*(4), 297–302. https://doi.org/10.1109/tct.1955.1085268

Neculai, A. (2008). An unconstrained optimization test functions collection. *Advanced Modeling and Optimization*, *10*, 147–61.

Palma, G., Bia, P., Mescia, L., Yano, T., Nazabal, V., Taguchi, J., et al. (2014). Design of fiber coupled Er^{3+}: Chalcogenide microsphere amplifier via particle swarm optimization algorithm. *Optical Engineering*, *53*(7). ID 071805. https://doi.org/10.1117/1.oe.53.7.071805

Pearson, L. W., & Wilton, D. R. (1981). Theorical aspects of the physical realizability of broad-band equivalent circuits for energy collecting structures. *IEEE Transactions on Antennas and Propagation*, *AP-29*(5), 697–707. https://doi.org/10.1109/tap.1981.1142649

Piro, G., Bia, P., Boggia, G., Caratelli, D., Grieco, L., & Mescia, L. (2016). Terahertz electromagnetic field propagation in human tissues: A study on communication capabilities. *Nano Communication Networks*, *10*, 51–59. https://doi.org/10.1016/j.nancom.2016.07.010

Rehman, O. U., Rehman, S. U., Tu, S., Khan, S., Waquas, M., & Yang, S. (2018). A quantum particle swarm optimization method with fitness selection methodology for electromagnetic inverse problems. *IEEE Access*, *6*, 63155–63163. https://doi.org/10.1109/access.2018.2873670

Rehman, O. U., Yang, S., Khan, S., & Rehman, S. U. (2019). A quantum particle swarm optimizer with enhanced strategy for global optimization of electromagnetic devices. *IEEE Transactions on Magnetics*, *55*, 1–4. ID 7000804. https://doi.org/10.1109/tmag.2019.2913021

Robinson, J., & Rahmat-Samii, Y. (2004). Particle swarm optimization in electromagnetics. *IEEE Transactions on Antennas and Propagation*, *52*(2), 397–407. https://doi.org/10.1109/tap.2004.823969

Streable, G. W., & Pearson, L. W. (1981). A numerical study on realizable broad-band equivalent admittances for dipole and loop antennas. *IEEE Transactions on Antennas and Propagation*, *AP-29*(5), 707–717. https://doi.org/10.1109/tap.1981.1142668

Sun, J., Fang, W., Palade, V., Wu, X., & Xu, W. (2011). Quantum-behaved particle swarm optimization with Gaussian distributed local attractor point. *Applied Mathematics and Computation*, *218*(7), 3763–3775. https://doi.org/10.1016/j.amc.2011.09.021

Sun, J., Feng, B., & Xu, B. W. B. (2004). Particle swarm optimization with particles having quantum behavior. In *Proceedings of the IEEE Congress on Evolutionary Computation*, (pp. 325–331).

Wing, O. (2008). *Classical circuit theory*. Springer.

Xi, M., Sun, J., & Xu, W. (2008). An improved quantum-behaved particle swarm optimization algorithm with weighted mean best position. *Applied Mathematics and Computation*, *205*(2), 751–759. https://doi.org/10.1016/j.amc.2008.05.135

Xu, Z., Fu, Z., & Zhang, J. (2020). Research and application of the transient electromagnetic method inversion technique based on particle swarm optimization algorithm. *IEEE Access*, *8*, 198307–198316. https://doi.org/10.1109/access.2020.3034441

Yurtkuran, A. (2019). *An improved electromagnetic field optimization for the global optimization problems*. Computational Intelligence and Neuroscience. ID 6759106.